

Chapter 4

Observed Properties of Boxy/Peanut/Barlens Bulges

Eija Laurikainen and Heikki Salo

Abstract We review the observed morphological, photometric, and kinematic properties of boxy/peanut (B/P) shape bulges. Nearly half of the bulges in the nearby edge-on galaxies have these characteristics, which fraction is similar to the observed bar fraction in Hubble types earlier than Scd. B/P bulges are generally detected in the edge-on view, but it has been recently demonstrated that barlenses, which are lens-like structures embedded in bars, are the more face-on counterparts of the B/P bulges. Multi-component structural decompositions have shown that B/P/barlens structures are likely to account for most of the bulge light, including the early-type discs harboring most of the bulge mass in galaxies. These structures appear in bright galaxies, in a mass range near to the Milky Way mass. Also the other properties of these bulges, including morphology (X-shaped), kinematics (cylindrical rotation), or stellar populations (old), are similar to those observed in the Milky Way. Cool central discs are often embedded in the B/P/barlens bulges. Barred galaxies contain also dynamically hot classical bulges, but it is not yet clear to what extent they are really dynamically distinct structure components, and to what extent stars wrapped into the central regions of the galaxies during the formation and evolution of bars. If most of the bulge mass in the Milky Way mass galaxies in the nearby universe indeed resides in the B/P-shape bulges, and not in the classical bulges, that idea needs to be integrated into the paradigm of galaxy formation.

4.1 Introduction

Galaxies in the nearby universe have complex morphological structures and indeed the concept of the bulge depends strongly on how we define it. Bulges can be considered simply as an excess flux above the disc, or they can be defined by detailed morphological, photometric, or kinematic properties. An important question is to what extent these central mass concentrations are associated to the early formative processes of galaxies, and how much are they modified via internal dynamical

E. Laurikainen (✉) • H. Salo
Astronomy and Space Physics, University of Oulu, FI-90014 Oulu, Finland
e-mail: eija.laurikainen@oulu.fi; heikki.salo@oulu.fi

processes. Using the notation by Athanassoula (2005) bulges are generally divided to *classical bulges*, *discy pseudobulges*, and *boxy/peanut (B/P) bulges*. Classical bulges are the most obvious imprints of galaxy formation at high redshifts, formed in some violent processes, followed by strong relaxation. They are structures supported by velocity dispersion, and also have centrally peaked surface brightness profiles with high Sérsic indexes. Pseudobulges are defined as structures formed by secular evolutionary processes out of the disc material. The concept of a pseudobulge was introduced by Kormendy (1982, 1983) who defined them as flat structures in the central parts of the discs, having excess of light above the disc in the surface brightness profile. Pseudobulges were later extended to include also the vertically thick boxy/peanut bulges, generally associated to bars (Athanassoula 2005; many B/Ps show also X-shape morphology). Since then the flat central mass concentrations have been referred as ‘discy pseudobulges’. A division of pseudobulges to these two categories is important, because their observed properties are very different.

The concept of a pseudobulge was created having in mind the relaxed universe where slow secular evolutionary processes are prevalent, not the early gas rich clumpy universe, or the universe where galaxy mergers dominate the evolution. However, it appears that similar internal mechanisms which take place in the local universe, like bar instabilities, can occur also at high redshifts, but in a much more rapid dynamical timescale. As discussed by Brooks and Christensen in Chap. 12 and by Bournaud in Chap. 13, at high redshifts also star formation and the different feedback mechanisms are faster and more efficient. All this can lead to the formation of pseudobulges even at high redshifts, for which reason associating the different bulge types to a unique formative process of bulge is not straightforward. In spite of that the above definition of bulges may still be a good working hypothesis at all redshifts, and give useful insight to the theoretical models.

This article reviews the observational properties of B/P bulges and also gives a historical perspective for the discovery of the phenomenon. The theoretical background of the orbital families is given by Athanassoula in Chap. 14. We have the following questions in mind: (a) what is the observational evidence that B/P bulges are vertically thick inner parts of bars and what are the relative masses of the thin and thick bar components? (b) Are the B/P structures the only bulges in galaxies with this characteristic, or do the same galaxies have also small classical bulges embedded in the B/P bulges? (c) What is our understanding of this phenomenon both in the edge-on and in face-on views? Although the topic is B/P bulges, connections are made also to other type of bulges if that is needed for understanding the phenomenon. Examples of boxy/peanut and X-shape bulges are shown in Fig. 4.1. The unsharp masks further illustrate the X-shape, which may appear weakly also in some bulges with apparent boxy appearance.

An outstanding recent discovery of the Milky Way (discussed in Chaps. 9 and 10 of this book) is that it harbors a boxy (Dwek et al. 1995) or even an X-shape bulge (Li and Shen 2012; Wegg and Gerhard 2013), covering most of the central mass concentration in our Galaxy. In fact, the model by Shen et al. (2010), explaining most of the observed properties of the Milky Way, does not have any classical bulge.

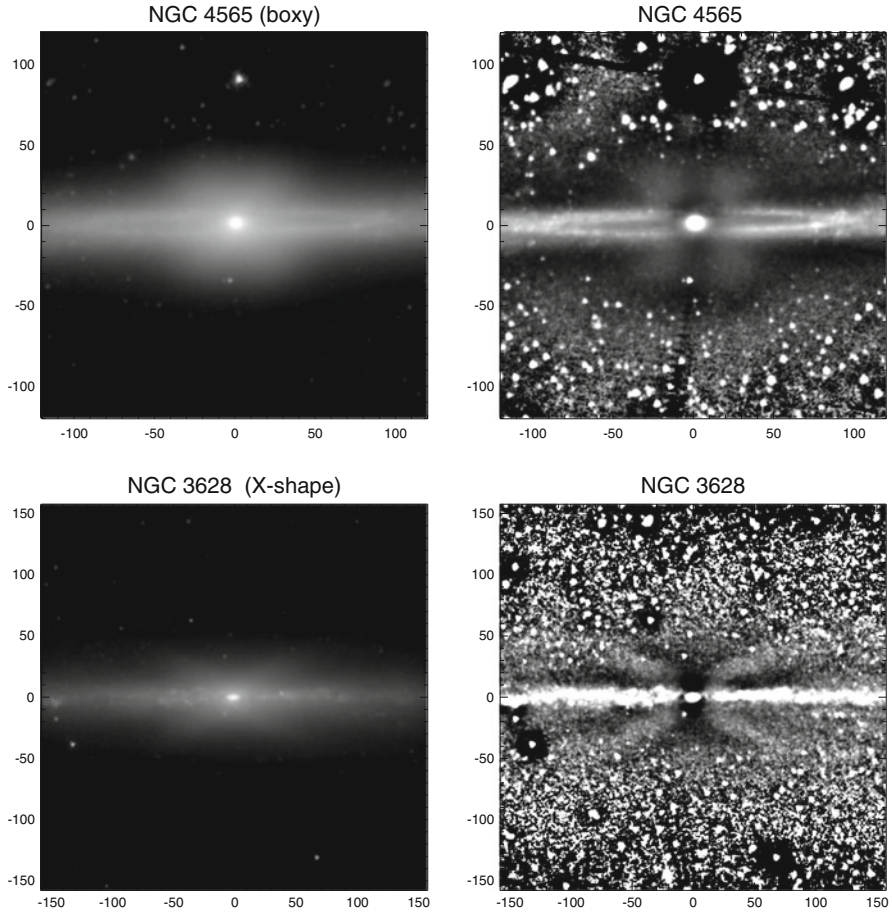


Fig. 4.1 Examples of boxy (NGC 4565) and peanut (NGC 3628) shape bulges, using the $3.6\ \mu\text{m}$ Spitzer space telescope images. Also shown are the unsharp mask images of the same galaxies, which in both galaxies show an X-shape morphology. The units of the x- and y-axis are in arcseconds

We will discuss observations which suggest that actually a large majority of the nearby galaxies in the Milky Way mass range might contain similar boxy or peanut shape bulges, where most of the bulge mass resides.

Good previous reviews of B/P bulges are those by Combes and Sanders (1981), Athanassoula (2005), and Debattista et al. (2006). Critical points in the interpretation of B/P bulges are given in the review by Graham (2011).

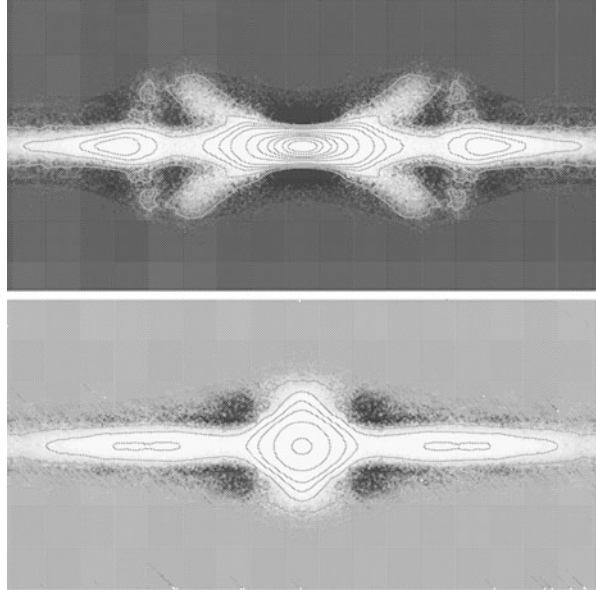
4.2 Discovery of B/P Bulges

The earliest notion of boxy bulges goes as far as to 1959, when the (Burbidge and Burbidge 1959) recognized such a structure in NGC 128, which galaxy was later shown in the Hubble Atlas of Galaxies by Sandage (1961). Some years later de Vaucouleurs (1974) paid attention to similar structures in some edge-on galaxies, at a time when bulges were generally thought to be like small ellipticals sitting in the middle of the disc. An interesting new explanation for the B/P bulges was given by Combes and Sanders in 1981: using N-body simulations they showed that when stellar bars form in galactic discs, in the edge-on view they reveal boxy or peanut shapes, similar to those seen in real galaxies. Soon after that a competing astrophysically interesting explanation for the formation of B/Ps was given by Binney and Petrou (1985), who suggested that they might be formed by violent or soft merging of satellite galaxies. Support for the scenario by Combes and Sanders came from the observation that NGC 4565 and NGC 128, with obvious boxy bulges in morphology, appeared to have cylindrical rotation (Kormendy and Illingworth 1982, 1983), which means that the rotational velocity depends only little on the vertical height from the equatorial plane. Kormendy and Illingworth argued that cylindrical rotation might actually be a typical characteristic of boxy bulges, but not of elliptical galaxies. It is also worth mentioning that Bertola and Capaccioli (1977) had already shown that the bulge in NGC 128 is fast rotating and therefore cannot be dynamically hot. However, it is worth noticing that not all bars seen end-on are perfectly round prolate structures.

After the first discoveries of B/P bulges in individual galaxies, systematic studies of B/Ps in galaxies seen in the edge-on view were carried out by Jarvis (1986) and Shaw et al. (1990). They suggested that B/Ps are concentrated to early-type disc galaxies (S0-Sab), and that peanuts are more common than boxy bulges, particularly in the late-type galaxies. They also showed evidence that galaxy environment (cluster/non-cluster, number of nearby companions) is not critical for the formation of the B/P bulges. These observations supported the idea that the B/P-structures indeed form part of the bar as suggested by Combes and Sanders (1981). However, this interpretation was not generally accepted at that time, partly because also 20 % of the elliptical galaxies appeared to be boxy (Lauer 1985). Bender et al. (1989) even speculated that boxy ellipticals might have a similar origin as the cylindrically rotating bulges in disc galaxies. Anyway, as the fraction of galaxies in which B/Ps were identified was only $\sim 20\%$, their exact interpretation would not significantly alter the estimated total mass fraction of classical bulges in the nearby universe.

This picture was changed by the studies of Dettmar and Barteldress (1988) and Lütticke et al. (2000a), based on more complete galaxy samples. Inspecting the isophotal contours of the galaxies they found that even 45 % of all S0-Sd galaxies

Fig. 4.2 Boxy/peanut bulges seen in the edge-on view in the simulation model by Athanassoula (2005, their figure 6): in the *upper panel* the line of sight is at 90° to the bar major axis, and in the *lower panel* the boxy/peanut is seen end-on (Reproduced with permission of Oxford University Press)



have B/Ps, which is already close to the fraction of barred galaxies: the somewhat larger number of detected bars ($\sim 50\text{--}60\%$) could be easily understood by the aspect angle of the bar. Namely, bars seen end-on view (along the bar major axis) would look like round structures, similar to the classical bulges (see the simulation model by Athanassoula 2005 in Fig. 4.2).

Lütticke et al. (2004) discovered also a new category of B/P bulges, the so called ‘thick boxy bulges’. Such bulges (see Fig. 4.3) are thought to be too extended to form part of the bar, and they also show asymmetries, or signs of recent mergers, which all means that they are not dynamically settled. Although they form only a minority of all B/Ps, they indicate that B/P bulges are not a uniform group of structures. In fact, in the prototype galaxy of ‘thick boxy bulges’, NGC 1055 (Shaw 1993), the bulge looks very much like a thick disc. This boxy bulge is rotating cylindrically, even in those regions of the observed light distribution where the bulge appears neither boxy nor peanut. Such rotation would be natural even if that structure were interpreted as a thick disc. This interpretation would be interesting, because in that case in traditional terms that galaxy barely has a bulge. In some galaxies even X-shape is visible in the ‘thick boxy bulge’ (Pohlen et al. 2004).

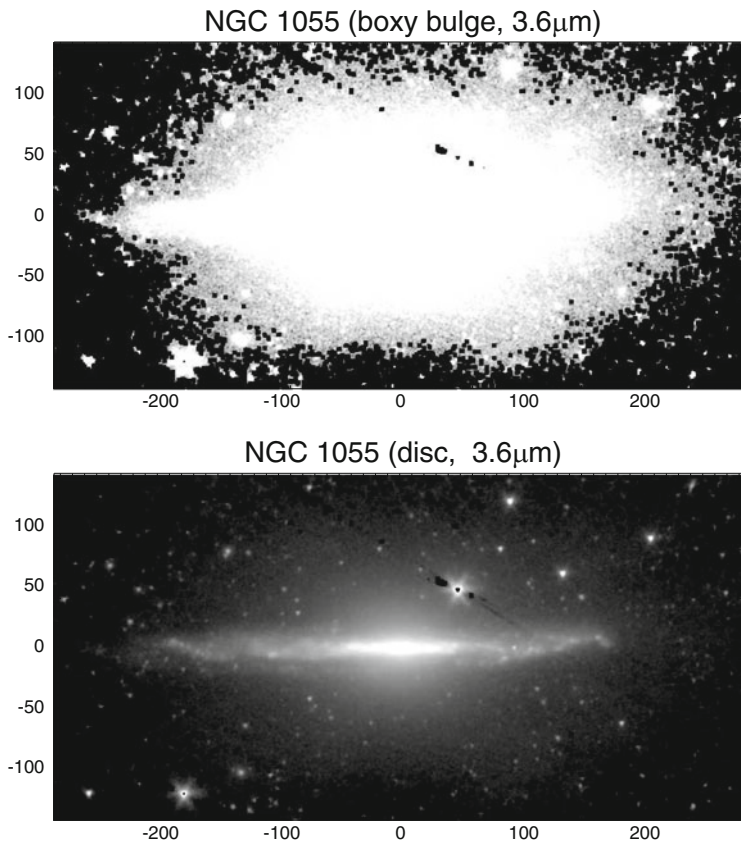


Fig. 4.3 NGC 1055, as an example of a thick boxy bulge. Shown is the $3.6\ \mu\text{m}$ Spitzer space telescope image in two different flux scales

4.3 Properties of the B/P Bulges in the Edge-On View

It was clear that more detailed analysis of the individual galaxies were needed, either to prove or disprove the possible bar origin of the B/P bulges. Such observations, particularly in the near-IR, where the obscuring effects of dust are minimal, were carried out by several groups. The observations were also compared with the predictions of the simulation models.

4.3.1 Direct Images

Morphology of the B/P-structures was systematically studied in the near-IR by Lütticke et al. (2000b). They were able to show that a large majority of these

structures can be associated with bars. In particular, they emphasized that the B/Ps are not just thick bars, but a combination of the vertically thick inner part of the bar, and a central bulge formed differently. They showed that the degree of the boxiness varies with the aspect angle of the bar, e.g. the bulge size normalized with barlength correlates with the level of boxiness of the bulge. These results were consistent with the predictions of the simulation models by Pfenniger and Friedli (1991), and they have been later confirmed by other simulations (Patsis et al. 2002a; Martínez-Valpuesta et al. 2006; Athanassoula and Misiouritis 2002; Debattista et al. 2005). Lütticke, Dettmar and Pohlen also measured the vertical thickness of the B/P, both in respect of barlength, and the size of the bulge (e.g. the size of the region with extra light above the exponential disc), in agreement with the predictions of the simulation models. The measured size of the B/P, normalized to barlength was ~ 0.4 , again in good agreement with the simulation models by Pfenniger and Friedli. Two possible explanations for the small central bulges were speculated by Lütticke et al. (2000b): they could be associated to the primordial bulges (i.e., ‘classical bulges’), or to the Inner Lindblad Resonance of the bar where a burst of star formation increases the mass concentration (i.e., ‘discy pseudobulges’). This idea has been recently renovated by Cole et al. (2014).

4.3.2 Unsharp Masks

The B/P bulges have been studied by Aronica et al. (2003) using unsharp mask images, which emphasize the sharp features that might appear in galaxies. They pointed out local surface brightness enhancements along the bar major axis on both sides of the bar, which enhancements appeared also in their simulation model after the bar had buckled. To illustrate this in Fig. 4.4 (upper panel) a comparison is made between a simulation model and the bar in ESO 443-042 observed at $3.6 \mu\text{m}$. In the same figure we show also a typical barred early-type galaxy, NGC 936, in almost face-on view. Also this galaxy has flux enhancements at the two ends of the bar, and it is tempting to argue that they are the same features as in ESO 443-042. We will come into this issue later.

Unsharp masks were used to study the B/P bulges also by Bureau et al. (2006), but now using a larger sample of 30 galaxies. In fact, in the study by Bureau et al. all the most important morphological characteristics of the B/P/X-shape structures for the edge-on galaxies are summarized, and are collected to our Figs. 4.4 and 4.5:

- (a) *Secondary maximum appears along the bar major axis* (upper row in Fig. 4.4), as discussed also by Aronica et al. (2003; see also Patsis et al. (2002a), their Fig. 5e).
- (b) *The X-shapes can be centered or non-centered*, e.g. the X-shape either crosses or does not cross the galaxy center (IC 2531 and NGC 4710 in Fig. 4.4).
- (c) *Minor-axis extremum appears* (NGC 1381 in Fig. 4.4), e.g., there is a rather narrow and elongated local maximum in the surface brightness profile along the minor axis near the galaxy center.

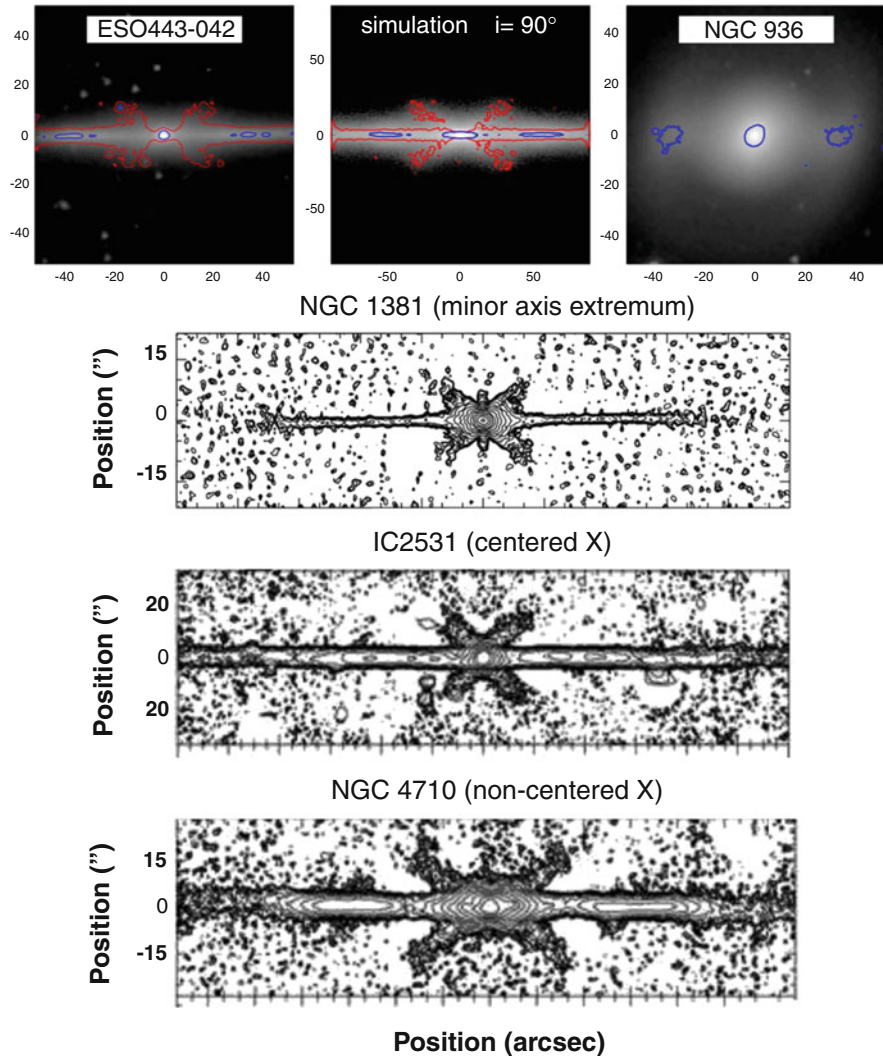


Fig. 4.4 The upper panel shows the Spitzer $3.6\ \mu\text{m}$ images for two galaxies with vertically thick inner bar components. For the edge-on galaxy ESO 443-042 it has an X-shape morphology, whereas in NGC 936 it appears as a barlens. Also shown is a simulation model (the same as in Fig. 4.10) in which the bar has buckled in the vertical direction. The contours denote the unsharp masks of the same images: *blue highlights* the brightest regions and *red color* the X-shapes. The lower panels show different X-shape morphologies in the edge-on view (Taken from Bureau et al. (2006). Reproduced with permission of Oxford University Press)

- (d) *Spiral arms* start from the two ends of the B/P (lower left panel in Fig. 4.5), e.g., symmetric, narrow, and elongated features appear, which on the two sides of the B/P are shifted with each other.

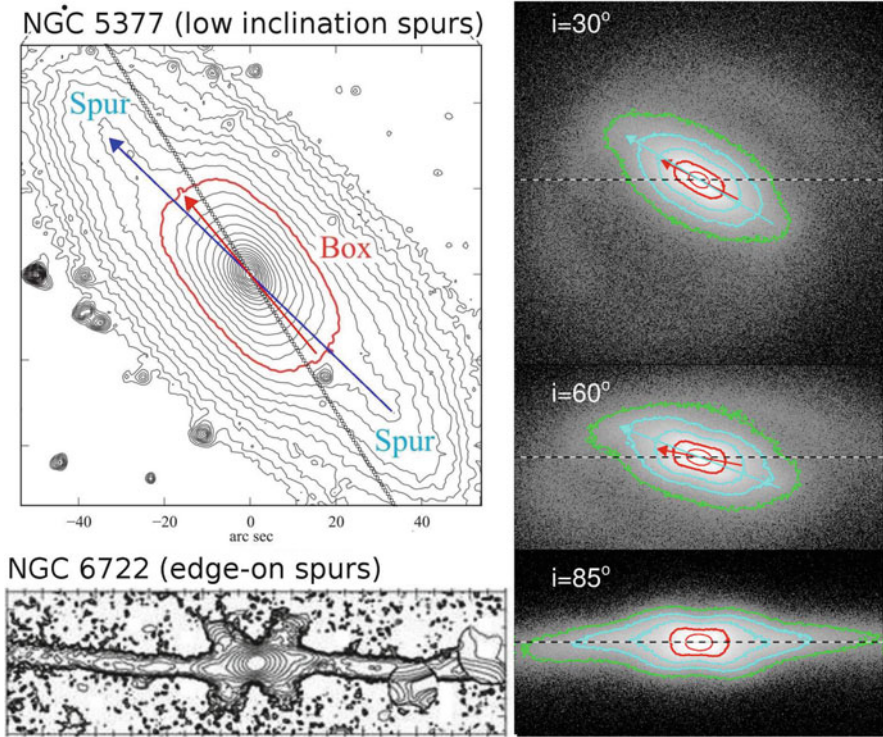


Fig. 4.5 Examples of barred galaxies with B/P-shape bulges at different viewing angles are shown. NGC 5377 shows isophotes from an archival Spitzer IRAC1 ($3.6\ \mu\text{m}$) image, and NGC 6722 is an unsharp mask of the K-band image. NGC 5377 has an inclination of 59° , whereas NGC 6722 is almost edge-on. The broad, nearly rectangular region in NGC 5377 is the boxy bulge, and the “spurs” projecting outside makes the outer part of the bar. As an inclination effect, in both galaxies the “spurs” or “spiral like features”, are twisted in respect to each other. *Arrows mark* their position angles, while the *dotted line* is the nodal line of the galaxy disc. Note how the position angle of the vertically thick boxy part falls between the position angles of the bar and the disc. *Right panels* show our simulations for a buckled bar (major axis makes a 35° angle with respect to nodal line), seen at different inclinations. The contours show the isophotes at different surface brightnesses, highlighting the inner and outer parts of the bar

The first two features are typical for the B/P bulges. According to Bureau et al. (2006) even 88 % of the galaxies with B/Ps have a secondary maximum along the bar major axis (in comparison to 33 % in their control sample). Also, 50 % and 38 % of the B/P bulges have off-centered and centered X-shapes, respectively (in 33 % in their control sample with no B/P structures). These features, as well as the minor-axis extremum, have been predicted also by the simulation models by Athanassoula (2005). Whether the X-shape is centered or not, in the models depends on the azimuthal angle of the bar: when viewed side-on the four branches

of the X-feature do not cross the center. However, for the centered X-shapes other explanations, like those related to galaxy interactions, have also been suggested (Binney and Petrou 1985; Hernquist and Quinn 1988; Whitmore and Bell 1988). Altogether, these comparisons showed that the most important characteristics in the morphology of the B/P bulges can be explained by bars.

Concerning the spiral arms, an overabundance in galaxies with B/P bulges was found by Bureau et al. (2006). As a natural explanation for that they suggested that the spiral arms are driven by bars, which is indeed predicted also by the dynamical models. However, it has not been convincingly shown how extended the bar driven spiral arms actually are (see Salo et al. 2010). In fact, looking at the images shown by Bureau et al. the structures that they call as spiral arms are very similar to the features called as ‘spurs’ by Erwin and Debattista (2013) in their recent study of more face-on barred galaxies (see upper left panel in Fig. 4.5). The ‘spurs’ can be understood as a combination of galaxy inclination, and the fact that the inner and outer parts of the bar have different vertical thicknesses. When the galaxy is not perfectly edge-on and the major axis of the bar makes an angle with respect of the nodal line, ‘spurs’ appear to be offset with respect to the major axis of the interior isophotes associated with the boxy bulge (see Fig. 4.5, middle right panel in our simulations). Using the words by Erwin and Debattista, “in an inclined galaxy projection of the B/P creates boxy isophotes which are tilted closer to the line of nodes than are the isophotes due to the projection of the other, flat part of the bar, which form the spurs”. Taking into account that not all galaxies in the sample by Bureau et al. are perfectly edge-on, in the two studies we are obviously speaking about the same phenomenon.

Lütticke et al. (2000b) left open the interpretation of the central peaks in the surface brightness profiles of the B/P bulges. However, Bureau et al. (2006) take a stronger view stressing that even the central surface brightnesses can be explained by the processes related to the formation and evolution of bars. They argue that classical bulges are not needed to explain their observations. As a support for this interpretation Bureau et al. showed that the surface brightness is more pronounced along the bar major axis than in the azimuthally averaged brightness, which was suggested to mean that most of the material at high vertical distances belongs to the B/P. In their view the steep inner peak in the surface brightness profile belongs to a flat concentrated inner disc (i.e., a ‘discy pseudobulge’ in our notation). Alternatively, the central peak belongs to the bar, formed as an inward push of the disc material when the bar was formed. In principle the colors would distinguish between these alternatives, but in the edge-on galaxies the central regions are contaminated by dust and stellar populations of the outer disc.

4.3.3 *Structural Decompositions*

Two edge-on galaxies with B/P bulges, NGC 4565 and NGC 5746, have been decomposed into multiple structure components by Kormendy and Barentine (2010)

and Barentine and Kormendy (2012). In the classification by Buta et al. (2015) the Hubble types of these galaxies are $SB_x(r)ab\ sp$, and $(R')SB_x(r,nd)0/a\ sp$. In direct infrared images the bulges in both galaxies clearly have boxy or even X-shape morphology. The surface brightness profiles were decomposed into an exponential disc, and two bulges (a ‘boxy bulge’ and a ‘discy pseudobulge’) fitted with separate Sérsic functions. In both galaxies the boxy bulges were assumed to be bars seen in nearly end-on view. For NGC 5746 there is also kinematic evidence for this interpretation, manifested as a ‘figure-of-eight’ line-of-sight velocity distribution, typical for boxy bars, which characteristic will be discussed in more detail in the next section.

An interesting outcome of these decompositions is that most of the bulge mass in these massive early-type disc galaxies resides in the boxy bulge. In NGC 4565 the boxy bulge-to-total mass ratio $B_{\text{boxy}}/T \sim 0.4$, and $B_{\text{discy}}/T \sim 0.06$ (i.e., a ‘discy pseudobulge’ in our notation). The 3.6 and 8 μm images and the decomposition for this galaxy are shown in Fig. 4.6. Both type of bulges are nearly exponential, along the major axis and perpendicular to that. A more simple decomposition for the same galaxy by Simien and de Vaucouleurs (1986), fitting only one de Vaucouleurs bulge ($n = 4$) and an exponential disc, leads to $B/T = 0.4$, which clearly corresponds to that obtained for the ‘boxy bulge’ by Kormendy and Barentine. Although the relative mass of bulge is practically the same in these two decompositions, the interpretation from the point of view of galaxy formation is totally different. This is one of those cases where the simple decomposition approach finds a classical bulge, although most of the bulge flux actually belongs to a boxy bar component. A key issue in the structural decompositions is that when there is a central peak in the surface brightness profile, and the various components of the disc are not fitted separately, leads to a massive bulge with large Sérsic index, typical for classical bulges.

Although a systematic study of the decompositions for B/P bulges seen in the edge-on view is still needed, the above discussed decompositions have already shown that there exist massive early-type spiral galaxies which have no classical bulges. Or, at least it is not self-evident how these tiny exponential central bulges should be interpreted.

4.3.4 Diagnostics of Bars in Gas and Stellar Kinematics

Although the B/P morphology can be easily recognized in the edge-on view, in most cases the images alone cannot tell whether those structures indeed form part of the bar or not. Bars in the edge-on view can be easily mixed with rings or lenses. Since the components might have different velocity dispersions which can be hotter than the underlying disc, kinematic tools to identify bars are important.

One such tool suggested by Kuijken and Merrifield (1995, see also Vega Beltran et al. 1997), is the ‘figure-of-eight’ structure in the line-of-sight velocity distribution (LOSVD) of galaxies, derived from the emission or absorption lines. It is based on

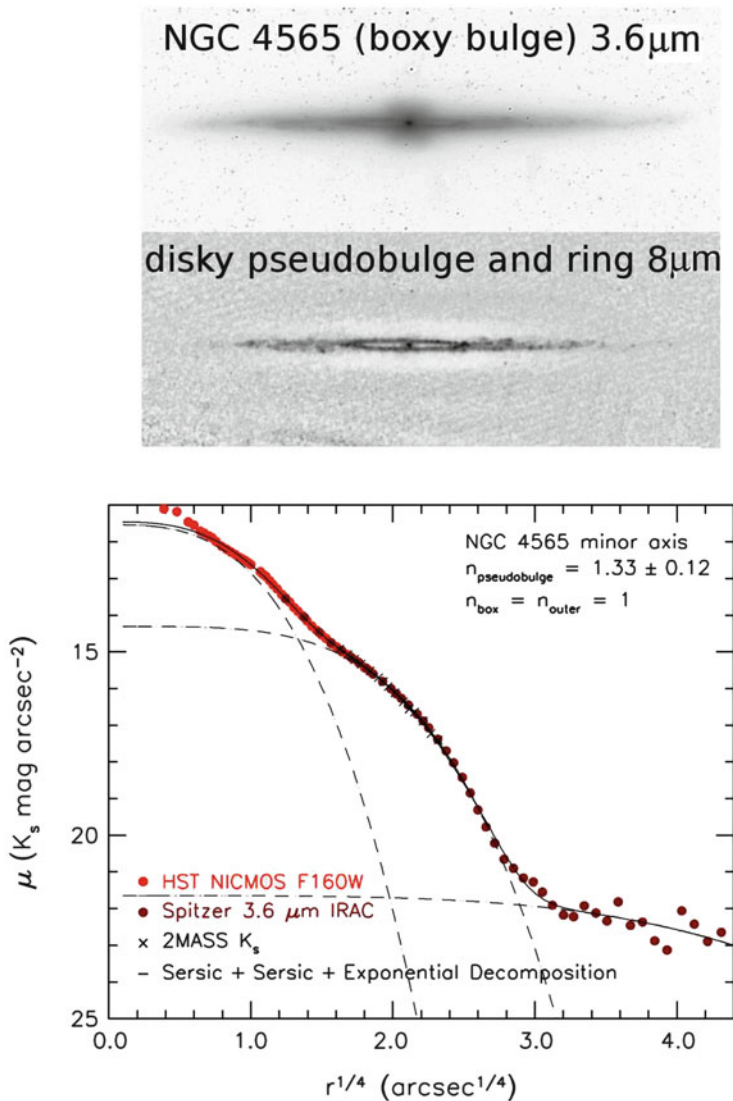


Fig. 4.6 Spitzer/IRAC 3.6 and 8 μm images of NGC 4565 (*upper and middle panels*) are shown to emphasize the boxy bulge, the ring and the tiny central pseudobulge. The *lower panel* shows a composite minor axis surface brightness profile made of the 3.6 μm image (*brown points*), and the Hubble space telescope image at F160W band (*red points*). The central pseudobulge and the boxy bulge are fitted with Sérsic functions and the outer structure with an exponential function. The *solid line* is the sum of the components. The nucleus is not fitted (The figure is taken from Kormendy and Barentine (2010), reproduced with permission of AAS)

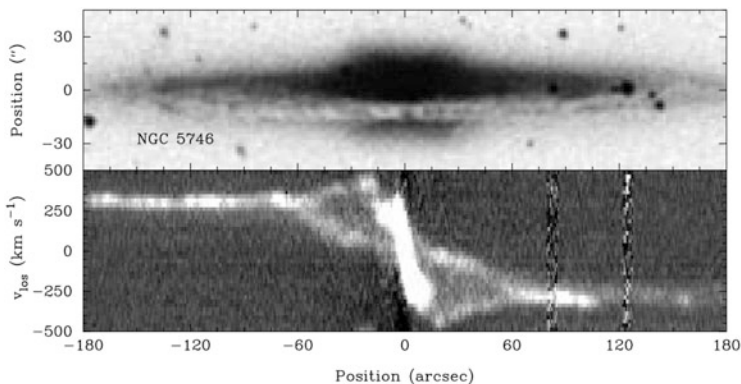
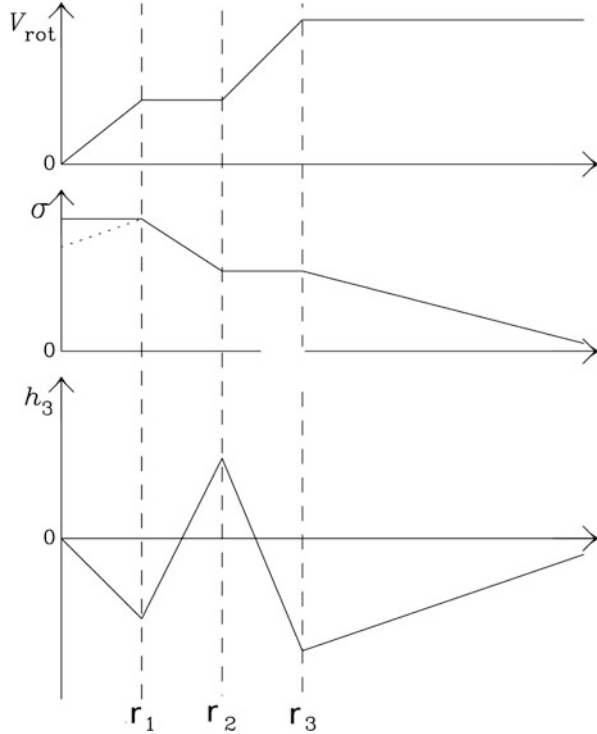


Fig. 4.7 The *upper panel* shows the K-band image of NGC 5746, and the *lower panel* the ionized gas [NII]6584 emission line position velocity diagram taken along the major axis (The figure is taken from Bureau and Freeman (1999), reproduced with permission of AAS)

the idea that the LOSVD has two peaks, one due to particles traveling in bar-related stellar orbits faster than the local circular velocity, and particles that travel more slowly than that. Variations in these velocities then form the ‘figure-of-eight’ in the diagram where the velocity is shown as a function of galaxy radius (see Fig. 4.7). A good correspondence of these observations with the predictions of the simulation models was obtained by Athanassoula and Bureau (1999), but soon it also became clear that this method works only for strong bars (Bureau and Athanassoula 2005).

The diagnostic tools were further developed by Chung and Bureau (2004, see also the review by Athanassoula 2005), with the main emphasis to distinguish, not only bars in general, but also the B/P bulges within the bars. The identification is based on inspection of the velocity (V_{rot}), the stellar velocity dispersion (σ), and the third and fourth terms of the Gauss-Hermite parameters along the major axis (see Bender et al. 1994), which measure the asymmetric (h_3) and symmetric (h_4) deviations of the LOSVD from a pure Gaussian. The h_3 parameter is expected to be a good tracer of the triaxiality of the bulge. The main diagnostics of bars with B/P bulges are shown in Fig. 4.8. They show ‘double humped’ rotation curves, flat-top or weakly peaked σ -profile, and that h_3 -profile correlates with V_{rot} over the projected bar length. Also h_4 -profile, although being a weaker indice, shows central and secondary minima. Chung and Bureau (2004) studied 30 edge-on spirals (24 with B/Ps) and showed that even 90 % of them showed kinematic signatures of bars. Not only bars were identified, but also the edges of the B/Ps were recognized in the h_3 -profiles. A large fraction (40 %) of those galaxies also showed a drop in the central velocity dispersion, being a manifestation of a dynamically cold central component.

Fig. 4.8 Schematic view of the main diagnostic tools to identify bars and B/P bulges. Shown are the radial profiles of the rotation velocity V_{rot} , the stellar velocity dispersion σ , and third Gauss-Hermite moment parameter h_3 . The vertical dashed lines indicate the radii of the central disc pseudobulge (r_1), boxy bulge (r_2) and the whole bar (r_3) (The figure is taken from Bureau et al. (2006). Reproduced with permission of Oxford University Press)



4.4 Detection and Properties of B/P-Shape Bulges in Face-On Systems

In face-on view the problem is the opposite: bars are easy to recognize in the images, but the B/P/X-shape structures, which are assumed to be thick in the vertical direction, presumably disappear in the face-on view. In fact, excluding the edge-on galaxies, the B/P-shape structures were expected to be visible only in a narrow range of galaxy inclinations near to the edge-on view. Nevertheless, using the words by Kormendy and Barentine (2010): “as long as face-on and edge-on galaxies appear to show physical differences we cannot be sure that we understand them.”

4.4.1 Isophotal Analysis

Isophotal analysis of the image contours has actually appeared to be a powerful tool to identify B/Ps in moderately inclined galaxies. This has been shown in a clear manner by Beaton et al. (2007) for M31 (see also Athanassoula and Beaton 2006 for simulations), which galaxy has an inclination of 77.5° . The main idea is to fit ellipses

to isophotes, and to measure the deviations from the elliptical shapes. The sine (A_4) and cosine (B_4) terms of the Fourier series measure the boxiness and disciness of the isophotes (see Fig. 4.9). In the boxy region B_4 is positive and A_4 is negative. Characteristic for the boxy region is also that the ellipticity increases towards the edge. On the other hand, the position angle is maintained constant throughout the bar region, at least for strong bars. The image of M31 is not shown here, but it would look very much like NGC 5377 in our Fig. 4.5, which galaxy has boxy inner isophotes associated to the boxy bulge, and ‘spurs’ associated to the more elongated part of the bar.

A similar analysis for a larger number of galaxies has been made by Erwin and Debattista (2013). They studied 78 barred S0-Sb galaxies, covering a large range of galaxy inclinations. The leading idea in their study was to find out an optimal range of galaxy inclinations ($i < 45^\circ$) and the bar’s position angles from the nodal line for the detection of B/P. Using a small parameter space they were able to study galaxies in which both the B/P bulge and the large scale bar could be identified in the same galaxies. This allowed also a more reliable estimate for the relative size of the B/P-structure ($R_{\text{boxy}}/R_{\text{bar}} \sim 0.4$), which appeared to be similar to that predicted by the simulation models of bars (Pfenniger and Friedli 1991; Athanassoula and Misiroidis 2002; Debattista et al. 2005), and is also similar to those obtained by Lütticke et al. (2000b) in observations. Also, extrapolating the number statistics of B/P bulges found in the ideal range of all bar/disc orientations and galaxy inclinations, they estimated that even 2/3 of bars might have B/P bulges. Taking into account that a certain fraction of bars at all inclinations must be end-on, this fraction is not far away from the suggestion made by Lütticke et al. (2000b) that all bars might have B/P structures. However, the extrapolation made by Erwin and Debattista for making their prediction is based only on a few galaxies with identified bars and B/P structures in the same galaxies.

A large majority of bars in the sample by Erwin and Debattista (2013) have boxy, rather than peanut-shape isophotes. A given explanation was that in the central regions of the B/P-structures there exist extra inner discs or compact bulges, which smooth out the peanut shape. In fact, the basic assumption in all the morphological and isophotal analysis of the B/P bulges discussed above is that the vertically thick inner parts of bars have either boxy or peanut shapes. However, based on the simulation models by Athanassoula et al. (2014) that is not necessarily the case in the face-on view where they can appear fairly round. In fact, the orbits populating the bars might have more complicated structures than just regular orbits around 3D bar-supporting periodic orbits (see Patsis and Katsanikas 2014a).

4.4.2 *Properties of Barlenses*

A different approach was taken by Laurikainen et al. (2011) who identified distinct morphological structures called barlenses, in a sample of ~ 200 early-type disc galaxies (NIRSOS atlas), observed at fairly low galaxy inclinations ($i \leq 65^\circ$).

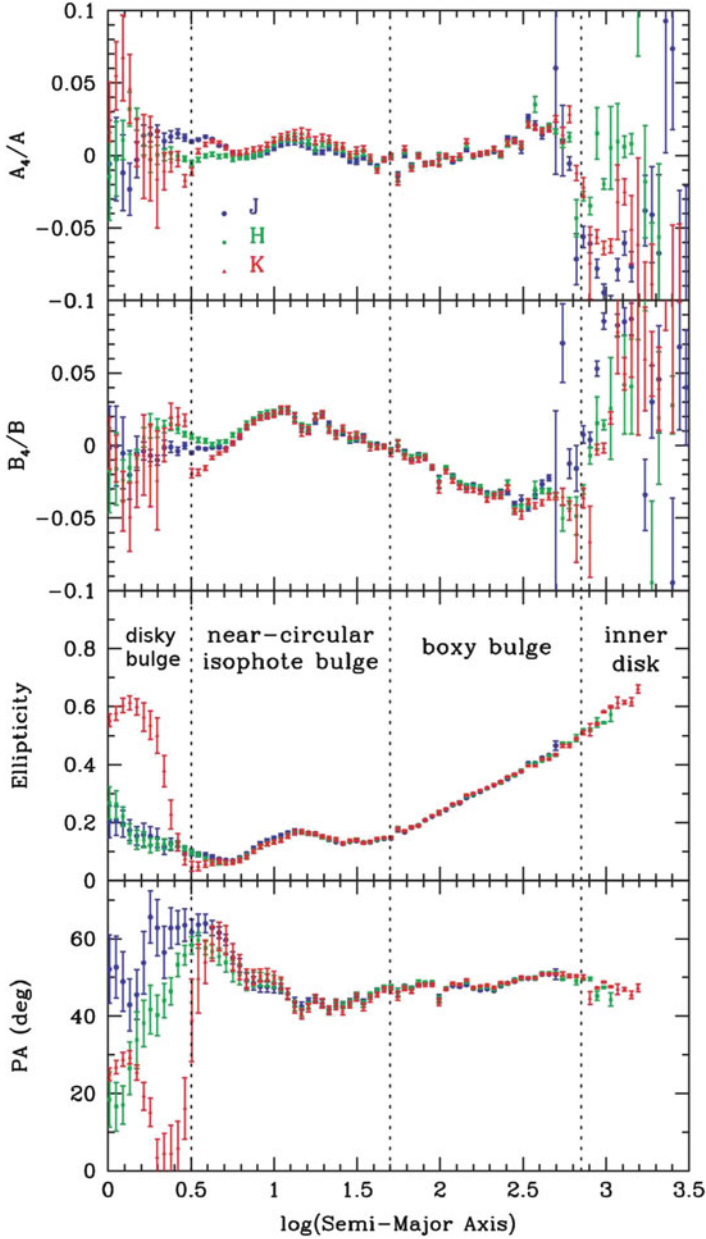


Fig. 4.9 Isophotal analysis of M31 which galaxy has a boxy bulge. Radial profiles (in arcseconds) of the ellipticities and position angles of the isophotes are shown in the *two lower panels*. The *upper panels* show the sine (A_4) and cosine (B_4) terms of the Fourier series of the same isophotes. Shown separately are the measurements in J, H and K-band bands. The regions covering the near-nuclear bulge ('disky pseudobulge' in our notation), boxy bulge, and inner disk (equivalent to 'spurs' in our Fig. 4.5) are shown by *dotted lines* (The figure is taken from Beaton et al. (2007), reproduced with permission of AAS)

Barlenses were recognized as lens-like structures embedded in bars, covering typically half of the barlength. In distinction to nuclear lenses they are much larger, and compared to classical bulges the surface brightness distribution decreases much faster at the edge of the structure. In Laurikainen et al. (2011) and in Buta et al. (2015) barlenses have been coded into the classification. These structures (though not yet called as such) were decomposed with a flat Ferrers function in many S0s already by Laurikainen et al. (2005). This kind of decompositions were summarized in Laurikainen et al. (2010). In Laurikainen et al. (2007) it was speculated that such inner lens-like structures might actually be the face-on views of the vertically thick B/P bulges. If barlenses indeed are physically the same phenomenon as the B/P bulges, that would make possible to have a consistent view of the relative masses of the classical and pseudobulges at all galaxy inclinations.

Two prototypical barlens galaxies, NGC 936 and NGC 4314, are shown in Figs. 4.4 and 4.10. In the images barlenses can be easily mixed with the classical bulges. However, in the surface brightness profiles barlenses appear as nearly exponential, flat sub-sections, both along the major and the minor axis of the bar. Characteristic morphological features for barlens galaxies are the ansae (or handles), which appear at the two ends of the bar (see NGC 936 in Fig. 4.4). It has been shown (Laurikainen et al. 2013) that even half of the barlenses are embedded in that kind of bars. In Sect. 4.3.2 we discussed that such flux enhancements are produced also in galaxy simulations, at the same time when the bar buckles in the vertical direction. This can be considered as further indirect evidence supporting the idea that barlenses indeed form part of a buckled bar. The unsharp mask image of NGC 4314 also shows a structure connecting the barlens to the more elongated part of the bar (see Fig. 4.10). Using the measurements in the NIRS0S atlas Athanassoula et al. (2014) showed that, in respect of the bar, barlenses have very similar sizes as obtained for the B/P bulges by Lütticke et al. (2000b) and Erwin and Debattista (2013).

Morphological structures similar to the observed barlenses are produced by N-body and smoothed particle hydrodynamical simulations by Athanassoula et al. (2013). In Athanassoula et al. (2014) detailed comparisons between the observations and models are shown. In their models barlenses appear in the face-on view without invoking any spheroidal bulge components in the initial models. An example of a barlens in such simulation model, seen both in the edge-on and face-on views, is shown in Fig. 4.10 (two lower left panels). Recent orbital analysis of bars by Patsis and Katsanikas (2014b) have shown that “sticky chaotic” orbits, building parts of bars can appear at high vertical distances in such a manner that when seen in the face-on view they form a boxy inner structure inside the bar (their fig. 8). These bar orbits might be the ones associated to barlenses in some cases. Whether also the X-shape is visible inside the boxy component depends on the specific combination of the orbital families of bars. A more thorough discussion of possible orbits making the barlens is given by Athanassoula in this book.

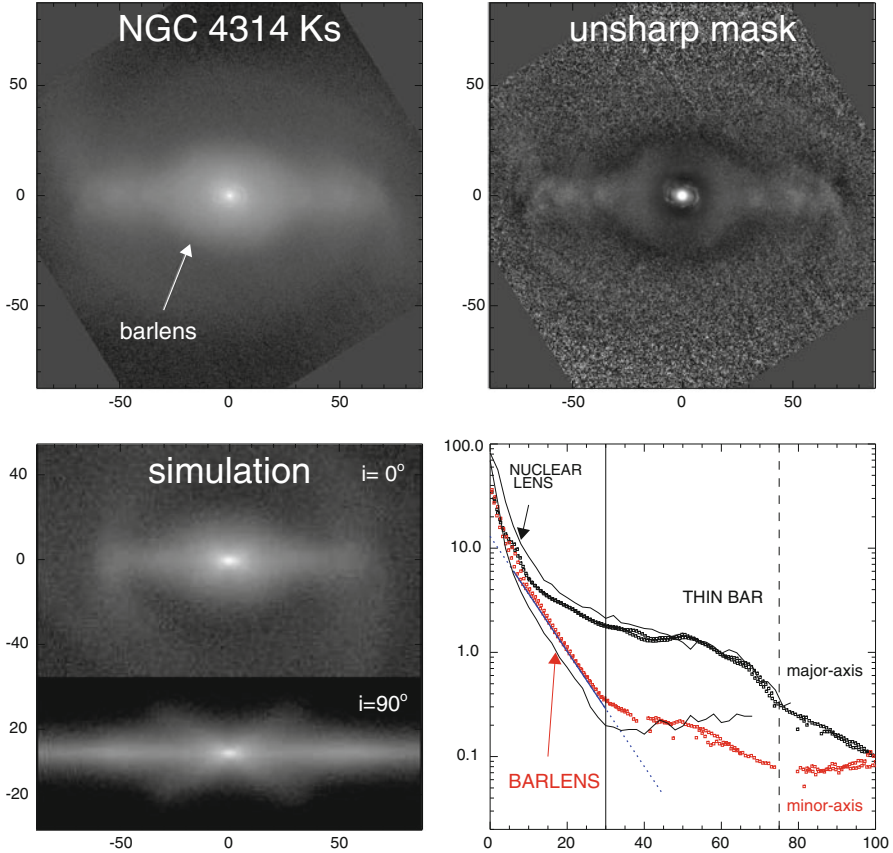


Fig. 4.10 An example of a barlens galaxy NGC 4314, showing the K_s -band image from Laurikainen et al. (2011; *upper left panel*) and the unsharp mask image of that (*upper right panel*). The surface brightness profiles along the bar major (*black symbols*) and minor axis (*red symbols*) are also shown. The *lower left panel* shows the simulation model gtr115 from Athanassoula et al. (2013, 2014), both in the face-on and edge-on view. The simulation model profiles are shown by *solid lines* in the profile plot. Axis labels are in arcseconds in all panels (The figure is taken from Laurikainen et al. (2014), reproduced with permission of Oxford University Press)

4.4.3 Barlenses: The Face-On Counterparts of B/P Bulges

If barlenses and B/P/X-shape bulges indeed were physically the same phenomenon, just seen at different viewing angles, we should see that in the number statistics in a representative sample of nearby galaxies. That has been looked at by Laurikainen et al. (2014) using a sample of 2465 nearby galaxies at 3.6 or 2.2 μm wavelengths, covering all Hubble types and galaxy inclinations (a combination of NIRS0S, and the Spitzer Survey of Stellar Structure of galaxies S⁴G). In order to find out all the X-shape structures unsharp masks were done for all these galaxies, in a similar

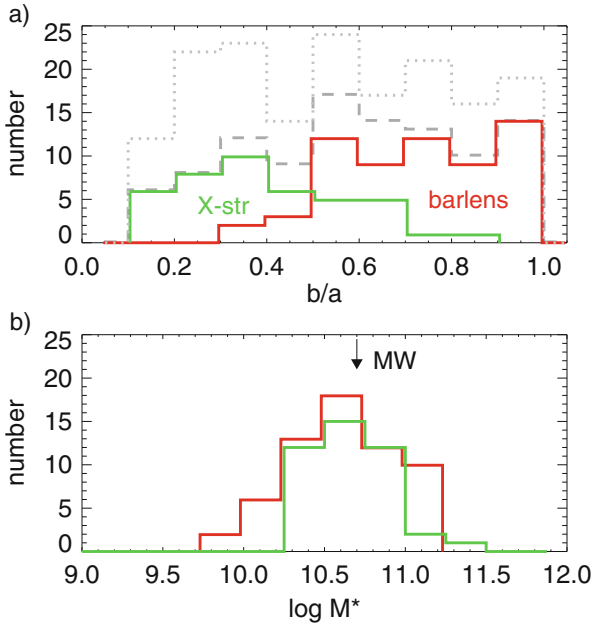


Fig. 4.11 The distributions of (a) galaxy minor-to-major (b/a) axis ratios and (b) total stellar masses (in units of solar masses) of the galaxies, hosting either barlens (red) or X-shape structures (green). In these plots a magnitude-limited ($B_r \leq 12.5$ mag) sub-sample of 365 barred galaxies in a combined S⁴G and NIRS0S is used. The grey dashed and dotted lines show the barlens and X-shapes structures, in the magnitude-limited sample and the complete S⁴G, respectively (Reproduced with permission of Oxford University Press)

manner as was done previously by Bureau et al. (2006) for a representative sample of edge-on galaxies. Barlens were recognized in the galaxy classifications of Buta et al. (2015) and Laurikainen et al. (2011). Remarkably, the apparent axial ratios of the galaxies with barlens and X-shape structures are consistent with a single population viewed from random orientations (Fig. 4.11, upper panel). Although barlens appear in less inclined galaxies, there is a large overlap in their parent galaxy inclinations, compared to those with X-shape structures. The parent galaxies of barlens and X-shape structures have similar distributions of total stellar mass (Fig. 4.11, lower panel), and also similar red colors. It is worth noticing that the peak in the mass distribution of these galaxies appears at the Milky Way mass. There are also similarities in the kinematics of barlens and X-shape structures, which will be discussed in Sect. 4.4.5.

It appears that among the S0s and early-type spirals even half of the barred galaxies have either a barlens or an X-shape structure, and $\sim 30\%$ if also the non-barred galaxies are included in the statistics (Laurikainen et al. 2014). This is not much less than the 45% of B/Ps found by Lütticke et al. (2000a) among the edge-on galaxies in the same morphological type bin. The slightly lower B/P fraction by

Laurikainen et al. can be explained by the fact that limiting to X-shape structures, most probably they picked up only the strong bars where the X-shapes are more pronounced (Athanasoula 2005). As Lütticke, Dettmar and Pohlen did not use any unsharp masks we don't know how many of the galaxies in their sample actually have X-shape structures. Most probably not all of them, because boxy isophotes can be identified in the edge-on view even if the bulges have no X-shapes. Fractions of B/Ps has been recently studied also by Yoshino and Yamauchi (2015) in a sample of 1700 edge-on galaxies in the optical region. In order to identify bars a comparison sample of 2600 more face-on galaxies was used. It was then assumed that the bar fraction is the same among the edge-on galaxies. They found that B/Ps appear in 20 % of the galaxies, which fraction is much lower than the 45 % found by Lütticke et al. (2000a). However, according to Yoshino and Yamauchi the fraction of B/Ps they found is very similar to that obtained by Lütticke, Dettmar and Pohlen if the weakest category of B/Ps by Lütticke et al. is omitted.

4.4.4 *Structural Decompositions*

The assumption that barlenses and B/P bulges are physically the same phenomenon allows us to estimate the relative masses of these components, since this can be done in a fairly reliable manner at moderate galaxy inclinations ($i \leq 65^\circ$) using multi-component decompositions. When the inclination of the disc increases, the reliability of these mass estimates rapidly decreases. The decompositions of Barentine and Kormendy (2012) discussed earlier were made to one-dimensional surface brightness profiles, which is indeed a reasonable approach for the galaxies in the edge-on view. However, applying a similar approach in a more face-on view, in particular when the bar has two components, would dilute the non-axisymmetric structure components, which would appear as one big bulge in the average surface brightness profile (in terms of the flux above the disc). A better approach is to fit the two-dimensional flux distributions of the galaxies.

Examples of the decompositions using a two-dimensional approach and fitting the two bar components separately, allowing also the parameters of the B/P/barlens to vary, are taken from Laurikainen et al. (2014). They used the $3.6 \mu\text{m}$ Spitzer images to decompose 29 nearby galaxies having either a barlens or an X-shape structure. The bulges (i.e., the central mass concentrations) and discs were fitted with a Sérsic function, whereas the two bar components were fitted either using a Ferrers or a Sérsic function. Representative examples of these decompositions are shown in Fig. 4.12. It appeared that the relative fluxes of barlenses and X-shape bulges form on average even 10–20 % of the total galaxy flux, in comparison to $\sim 10\%$ in the central bulges (i.e., a 'discy pseudobulges'). In IC 5240 (Sa) the only bulge seems to be the X-shaped bar component. On the other hand, NGC 4643 (S0⁺) might have also a small central bulge embedded in the barlens. Looking at the surface brightness profile alone we don't know for sure whether the central peak is really a distinct bulge component, or is it rather formed of the same material as

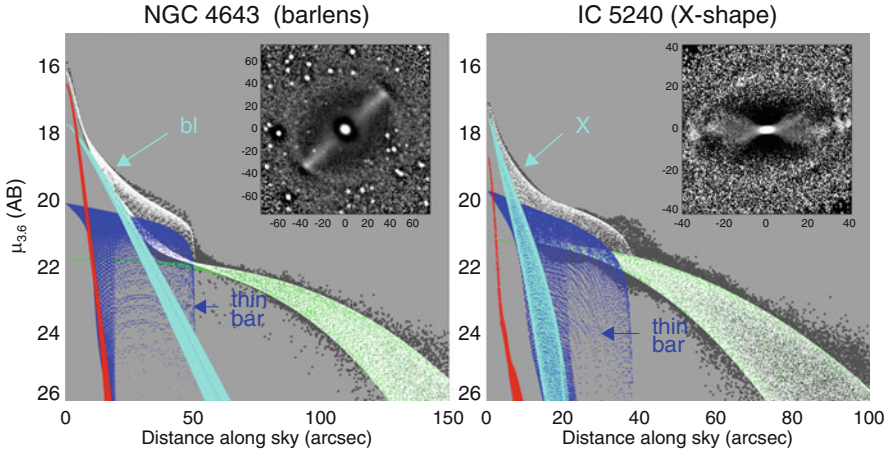


Fig. 4.12 Decomposition models for the barlens and X-shaped galaxies NGC 4643 and IC 5240, which are barred galaxies with Hubble stages $S0^+$ and Sa, respectively. The unsharp mask images are shown in the small *inserts* in the upper corners. *Black dots* are the pixel values of the two-dimensional flux-calibrated $3.6\ \mu\text{m}$ Spitzer images, and *white dots* show the pixel values of the total decomposition models. *Red* and *green dots* show the bulge and the disc components, whereas the *dark* and *light blue* indicate the thin and thick bar (i.e., the barlens and X-shape structure) components (The figure is taken from Laurikainen et al. (2014), reproduced with permission of Oxford University Press)

the rest of the bar, at the epoch of bar formation. The Sérsic index of the central component is $n = 0.7$ indicating that it is not a classical bulge. One possibility is that it is a manifestation of an old pseudobulge formed at high redshift, composed of old stars. That kind of pseudobulges form in the hydrodynamical cosmological simulations by Guedes et al. (2013), via a combination of disc instabilities and minor mergers.

If the B/P bulges (i.e., the barlenses or X-shape structures in the above decompositions) are omitted in the decompositions that would dramatically affect the obtained relative masses of the classical bulges. In the early-type disc galaxies the deduced central bulge will increase from 10 % to 35 % in the sample by Laurikainen et al. (2014), the value 35 % being consistent with the previous more simple bulge/disc/bar decompositions (Gadotti 2009; Weinzirl et al. 2009). In Sect. 4.3.3 we discussed an edge-on galaxy, NGC 4565, for which galaxy the same happens when the simple and more detailed decompositions are compared.

We can compare the decompositions by Laurikainen et al. (2014) with those obtained by Erwin et al. (2003) for NGC 2787 and NGC 3945. Using a completely different decomposition approach they ended up with similar small relative masses for the central bulges in these two galaxies, just different names were used for the bulges. What is a barlens in Laurikainen et al. (2014), is called as an inner disc by Erwin et al., which discs are a magnitude larger than the central classical bulges, manifested as peaks in the surface brightness profiles. Similar approach

as in Erwin et al. (2003) has been recently taken also by Erwin et al. (2015) for additional seven barred early-type galaxies, but now calling the “inner discs” as “discy pseudobulges”. They identified boxy isophotes only in one of those galaxies, but many of them are classified as having a barlens by Laurikainen et al. (2011).

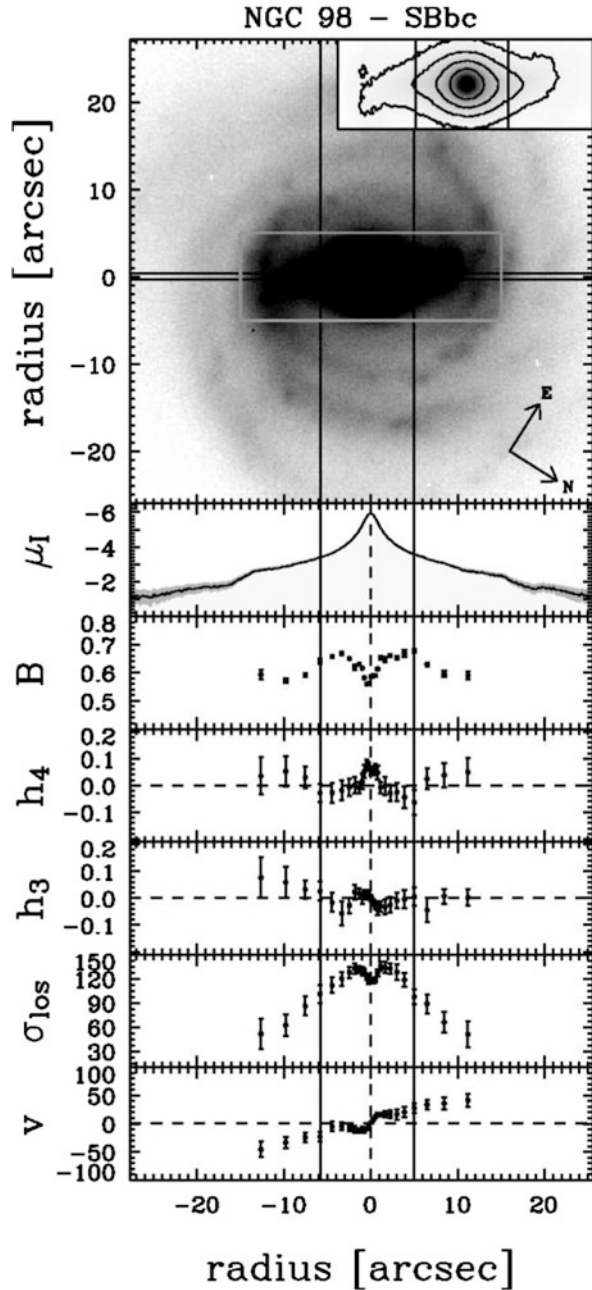
The small central B/P bulges are indeed intriguing, and the obtained nature of those bulges depends on how they are interpreted. As discussed by Chung and Bureau (2004), and more recently by Mendez-Abreu et al. (2014), cool disc components manifesting as nuclear rings or spiral arms, are often embedded in the B/P bulges. An example of a barlens galaxy with similar characteristics is NGC 4314, showing a star forming nuclear ring inside the boxy bulge. However, at least in the near-IR these central cool components are expected to contribute very little in the surface brightness profiles.

4.4.5 Diagnostics of B/P Bulges of Stellar Kinematics

Using simulation models an attempt to identify B/P structures in more face-on galaxies was done by Debattista et al. (2005). The diagnostics largely relies on the analysis of the fourth-order Gauss-Hermite moment, h_4 along the bar major axis. A B/P bulge is recognized as negative double minima in the h_4 -profile. These minima appear because the vertical velocity distribution of stars becomes broader, for which reason h_4 is a good proxy for the unobservable vertical density distribution. However, in spite of the smart idea, this method has been applied only for a few galaxies with B/P bulges, like NGC 98 (Méndez-Abreu et al. 2008). The reason is that the observations are very demanding and require a large amount of observing time at large telescopes. The diagnostics for NGC 98 is shown in Fig. 4.13. The size of the B/P is estimated from the radius of the minimum in the h_4 -profile, which in this case is 0.35 times the bar semi-major axis length. The same diagnostics has been recently applied for ten more face-on barred galaxies by Mendez-Abreu et al. (2014). They identified B/P bulges in two additional galaxies, and marginally in three more galaxies. In four of these galaxies a dynamically cool central component inside the B/P bulge was the only central bulge, without any sign of a dynamically hot classical bulge.

In the above studies long-slit spectroscopy was used. In principle integral-field unit (IFU) spectroscopy would be ideal to trace the B/P/X/barlens features, but the resolution and the field-of-view have not yet been sufficient for very detailed studies of B/Ps (see the review by Falcon-Barroso in Section 7). So far the largest survey using IFU spectroscopy is the ATLAS^{3D}, in which 260 nearby early-type galaxies, at all galaxy inclinations, have been mapped within one effective galaxy radius (Cappellari et al. 2007; Emsellem et al. 2011). Almost all bulges (86 %) were found to be fast rotating, which is consistent with the idea that most of the bulge mass in the nearby galaxies resides in the B/P/barlens bulges, rotating with the underlying disc (see Laurikainen et al. 2014). Most probably due to the limitations of the observations only a small fraction (15 %) of the fast rotating bulges showed

Fig. 4.13 Morphology and stellar kinematics of NGC 98. The *top panel* shows the I-band image, where the slit position and image orientation are also indicated. The *inset* shows the portion of the galaxy image marked with a *white box*. The panels show from top to bottom the radial profiles of surface brightness, broadening parameter B, fourth (h_4) and third (h_3) moments of the Gauss-Hermite series, line-of-sight velocity dispersion (σ_{los}), and the stellar velocity v . The *two vertical lines* indicate the location of the h_4 minima associated with the B/P region in NGC 98 (The figure is from Méndez-Abreu et al. (2008). Reproduced with permission of AAS)



signatures of B/P-structures, in terms of double peaked rotation curves or twisting isophotes (see Krajnovic et al. 2011).

We used the Atlas3D in the following manner. We picked up all those barred galaxies that have either a barlens or an X-shaped structure identified in the images in the sample by Laurikainen et al. (2014), and then looked at what kind of kinematics the Atlas3D finds for those galaxies. We found 27 galaxies in common between the two surveys (11 with X-shapes, 16 with barlenses). It appeared that all these galaxies are classified as regular fast rotators in Emsellem et al. (2011). Half of them have ‘double humped’ rotation curves, indicative of B/P-structures, but the other half has no particular kinematic features of which the vertically thick bar components could be identified. It is interesting that the fractions of the double humped rotation curves are fairly similar among the galaxies having barlenses and X-shaped structures (56 % and 36 %, respectively), which fractions are much higher than for the bulges in the Atlas3D in general. This is consistent with the idea that barlenses and B/P bulges are manifestations of the same physical phenomenon.

From the point of view of galaxy formation, the interpretation of bulges is complicated because internal dynamical effects in galaxies might modify the kinematic properties of bulges. For example, it has been suggested by Saha et al. (2012) that a small bulge embedded in a bar can absorb angular momentum from the bar, with a consequence that an initially non-rotating classical bulge can transform into a cylindrically rotating triaxial object. Saha and Naab (2013) have also suggested that the appearance of B/P bulges might be connected to the properties of dark matter halos.

4.5 Stellar Populations of B/P Bulges

Stellar populations of bulges in barred and non-barred galaxies have been compared using both absorption line-indices and applying stellar population synthesis methods, but no clear conclusions are derived. Using line-indices for 20 fairly face-on early-type barred galaxies and comparing them with the non-barred galaxies by Moorthy and Holzman (2006), Pérez and Sánchez-Blázquez (2011) found that bulges in barred galaxies are more metal-rich and more α -enhanced than in non-barred galaxies. The α -enhancement is associated to rapid star formation event, which is not expected if bulges formed via vertical buckling during the formation and evolution of bars. Synthetic stellar population methods has been applied for 62 barred and non-barred galaxies by Sánchez-Blázquez et al. (2014), also for fairly face-on galaxies. However, no difference in metallicity or age gradients between barred and non-barred galaxies were found. A sample of 32 edge-on galaxies was studied by Jablonka et al. (2007), and again no difference in the stellar populations of bulges was found between barred and non-barred galaxies.

From our point of view critical questions are do the barred galaxies in the above samples have B/P/barlens bulges or not, and what was measured as a ‘bulge’. For the first sample detailed morphological classifications exist for 10 galaxies and it

appears that even half of those have barlenses in Laurikainen et al. (2011). In the second sample 11 barred galaxies have detailed classifications, but none of them have neither B/P nor barlens. In Pérez and Sánchez-Blázquez (2011) the bulges were taken to be the central regions of the galaxies, which means also central regions of barlenses. In most of the bulges studied by them star forming nuclear rings and spiral arms were detected. In these fairly face-on galaxies the star forming structures obviously had a strong impact on the obtained stellar populations and metallicities, and do not tell about the main stellar population of the B/P bulges. It was pointed out already by Peletier et al. (2007) that composite bulges in stellar populations indeed exist. And also, that due to dust in the disc plane, at least in the optical region, the stellar populations and metallicities in the edge-on and face-on views are expected to be different.

Clearly, understanding the different bulge components calls for detailed studies of individual galaxies. Based on the analysis of four early-type galaxies Sánchez-Blázquez et al. (2011) showed that most of the stars in bulges are very old (10 Gyr), as old as in the Milky Way bulge. The same is true for bars, in which the stellar population ages are closer to the bulges than to the discs outside the bars (Pérez et al. 2009). The stellar populations of the B/P bulges in 28 edge-on early-type disc galaxies (S0-Sb) have been studied by Williams et al. (2011, 2012), and compared with the elliptical galaxies. They looked at the properties both in the central regions, covering the seeing-limited part of the boxy bulge, and in the main body of the B/P structures. The central peaks were found to have similar old stellar populations and high stellar velocity dispersion as in elliptical galaxies. However, the main body of the B/P bulge lacks a correlation between the metallicity gradient and σ , which correlation appears in elliptical galaxies. Metallicity gradients are easily produced in a monolithic collapse in the early universe, and at some level also in violent galaxy mergers. But even the non-barred galaxies in their study appeared to have stronger metallicity gradients than the B/P bulges of the same galaxy mass.

In the literature it is often argued that the stellar populations of bulges in S0-Sbc galaxies are similar to those of the elliptical galaxies (Proctor and Sansom 2002; Falcón-Barroso et al. 2006; MacArthur et al. 2009), which similarity breaks only in the later type spirals (see Ganda et al. 2007). However, based on the analysis by Williams et al. (2012), whether the bulges are similar to the ellipticals or not, depends on what do we count as a bulge. If we mean the central peaks in the radial flux distributions, then the answer is that the bulges indeed are much like the elliptical galaxies, but if we are talking about the main body of the B/Ps, then the stellar populations are different from the elliptical galaxies.

An interesting example is NGC 357 (de Lorenzo-Cáceres et al. 2012) for which galaxy all critical diagnostics of B/P-structures have been made, including the isophotal and stellar population analysis, kinematics, and structural decompositions. They found that no single unambiguous interpretation can be given for the bulge. The galaxy has two bars, which further complicates the interpretation. This example demonstrates that based on the same analysis completely different interpretations can be given for the bulge, depending on whether only the central peak, with high rotation and σ drop, is considered as a bulge (i.e., a ‘discy pseudobulge’ in

our notation), or the larger region with high σ is taken to be the bulge (i.e., the classical bulge in our notation). In their view, a problem in the first interpretation is that the bulge has an old stellar population, generally not accepted for a ‘discy pseudobulges’. If a classical bulge is assumed then the problem is the nearly exponential surface brightness profile. If the bulge is interpreted as a classical bulge then there exists also a cool central disc inside that bulge.

But for the interpretation of this particular galaxy there exists also a third possibility, namely that there is a boxy bulge and a central cool disc embedded in that. In this fairly face-on galaxy no B/P is identified in the isophotal analysis, but the galaxy looks very much like NGC 4643, in which galaxy a barlens has been recognized (see Laurikainen et al. 2014). The main bulge with the old stellar population and a small Sérsic index could simply correspond to the boxy bulge, which can also be dynamically fairly hot. The σ drop could be associated to a central cool disc embedded in the boxy bulge. It is worth noticing that the bulge has similar V-H color as the rest of the galaxy, up to the outer radius of the bar (Martini et al. 2003), which fits into this interpretation. However, the purpose of this paragraph is not to give the ‘right interpretation’, but rather to demonstrate that not only detailed observations are needed to study the bulges, but also the interpretation depends on the current understanding of bulges.

4.6 Summary and Discussion

Nearly half of the highly inclined galaxies in the nearby universe are found to have B/P/X-shape bulges. Barlenses, which appear in more face-on galaxies, are likely to be physically the same phenomenon. These structures appear in bright galaxies, in a mass range near to the Milky Way mass. Also the other properties of these bulges, including morphology (B/P/X-shape), kinematics (cylindrical rotation or double humped rotation curves), and stellar populations (old), are similar to those observed in the Milky Way. Cool central discs are often embedded inside the B/P/barlens bulges, in which case they are called as composite bulges. Barred galaxies with composite bulges can contain also dynamically hot classical bulges, but it is not yet clear to what extent they, in the Milky Way mass galaxies, are really dynamically distinct structure components, and to what extent stars wrapped into the central regions of the galaxies during the formation and evolution of bars.

A comparison of the observed properties of B/P/barlens bulges with the simulation models have shown that they can indeed be explained as disc structures, possibly formed by buckling instabilities soon after the bars were formed. It is unlikely that any significant fraction of B/P bulges were triggered by tidal effects. Independent of the exact isophotal shapes, these structures typically cover nearly half of the bar size, but can be also smaller or larger than that. Also, recent structural multi-component decompositions have shown that most of the bulge mass in these galaxies might appear in the B/P/barlens bulges. The exceptions are the boxy structures appearing in the most massive ($M > 10^{11} M_{\odot}$) slowly rotating galaxies,

which are often elliptical galaxies (sometimes S0s) in classification. Exceptions are also the ‘thick boxy bulges’, which might actually be manifestations of thick discs in the otherwise almost bulgeless galaxies.

If we believe that most of the bulge mass in the Milky Way mass galaxies indeed appears in the B/P/barlens bulges, it means that the masses of the classical bulges must be very low in all Hubble types, even in the early-type disc galaxies which are usually assumed to contain most of the baryonic spheroidal mass. If we are unwilling to accept this conclusion, then it needs to be explained how the observed morphological and kinematic properties of the B/P/X-shape/barlens bulges are created in galaxies. Why is this view then not accepted as a paradigm in the astronomical community? Actually, the argument that the B/P bulges form part of the bar, has been accepted, but perhaps not the idea that such bar components could contain most of the bulge mass in the Milky Way mass nearby galaxies. One possible reason for that is that the relative masses of bulges are generally estimated from decompositions performed for fairly face-on systems, in which galaxies the massive, round components are often erroneously interpreted as classical bulges.

The explanations discussed for the formation of pseudobulges in this review are related to the evolution of bars. A natural question is then what makes the bulges in the non-barred galaxies? If barred and non-barred galaxies live in similar galaxy environments also the accretion events should be similar, leading to bulge masses not too different from each other. The relative masses of bulges in barred and non-barred galaxies are compared for S⁴G sample (Sheth et al. 2010) of 2350 galaxies at 3.6 μm by Salo et al. (2015). For galaxies brighter than $M^* > 10^{10} M_{\odot}$ larger bulge masses were found for barred galaxies ($B/T \sim 0.15$ and $B/T \sim 0.09$, respectively). Since in this study a photometric definition of a ‘bulge’ was used (excess flux above the disc in the surface brightness profile), this difference most probably reflects the fact that in barred galaxies part of the apparent bulge mass is associated to the B/P/barlens bulge. Also, there is some observational evidence that even in the non-barred galaxies the bulges might have a B/P/barlens origin, once the thin part of the bar has been dissolved (see Laurikainen et al. 2013). The orbital analysis by Patsis et al. (2002b) also predicts that peanuts may form even in galaxies without creating any elongated, vertically thin bar components. Naturally, there exist also other ways of making pseudobulges in the non-barred galaxies, of which minor mergers are one of the most prevalent (see Eliche-Moral et al. 2013).

As a concluding mark we can say that in order to fully understand bulges the same formative processes need to be valid both in the edge-on and in face-on views. Also, it has become evident that bulges are complex systems so that detailed studies of individual galaxies are needed to separate the different bulge components. But even in that case, the interpretation always reflects also the prevalent theoretical understanding of a bulge, regardless of how sophisticated diagnostics are used.

Zu dem gebrauchten sowohl, wie zum dumpfen und stummen Vorrat der vollen Natur, den unsäglichen Summen, zähle dich jubelnd hinzu und vernichte die Zahl.

Acknowledgements We acknowledge the constructive comments from the referee. We also acknowledge the DAGAL Marie Curie Initial Training Network and the financial support from the Academy of Finland.

References

- Athanassoula, E. 2005, *MNRAS*, 358, 1477
- Athanassoula E., and Beaton, R. 2006, *MNRAS*, 370, 1499
- Athanassoula, E., Machado, R., and Rodionov, S. A. 2013, *MNRAS*, 429, 1949
- Athanassoula, E., Laurikainen, E., Salo, H., and Bosma, A. 2014, *astro-ph* 1405.6726
- Athanassoula, E., and Bureau, M. 1999, *ApJ*, 522, 699
- Athanassoula, E., and Misiornitis, A. 2002, *MNRAS*, 330, 35
- Aronica G., Athanassoula, E., Bureau, M., Bosma, A., Dettmar, R.-J., Vergani, D., and Pohlen, M. 2003, *ApSS*, 284, 753
- Barentine J., and Kormendy, J. 2012, *ApJ*, 754, 140
- Beaton, R., Majewski, S., Guhathakurta, P. Skrutskie, M. F., Cutri, R. M., Good, J., Patterson, R. J., Athanassoula, E., and Bureau, M. 2007, *ApJ*, 658, 91
- Bertola, F., and Capaccioli, M. 1977, *ApJ*, 211, 697
- Bender, R., Surma, P., Doebereiner, S., Moellenhoff, C., and Madejsky, R. 1989, *A&A*, 217, 35
- Bender, R., Saglia, R., and Gerhard, O. 1994, *MNRAS*, 269, 785
- Binney, J., and Petrou, M. 1985, *MNRAS*, 214, 449
- Burbidge, G., and Burbidge, M. 1959, *ApJ*, 130, 20
- Bureau, M., and Freeman, K. 1999, *AJ*, 118, 126
- Bureau, M., and Athanassoula, E. 2005, *ApJ*, 626, 159
- Bureau, M., Aronica, G., Athanassoula, E., Dettmar, R.-J., Bosma, A., and Freeman, K. C. 2006, *MNRAS*, 370, 753
- Buta, R. Sheth, K., Athanassoula, E., Bosma, A., Knapen, J., Laurikainen, E., Salo, H. et al. 2015, *ApJS*, 214, 32
- Cappellari, M., Emsellem, E., Bacon, R. Bureau, M., Davies, R. L., de Zeeuw, P. T., Falcón-Barroso, J. et al. 2007, *MNRAS*, 379, 418
- Cole, D., Debattista, V. P., Erwin P., Earp, S., and Roskar, R. 2014, *MNRAS*, 445, 3352
- Combes, F., and Sanders, R. H. 1981, *A&A*, 96, 164
- Chung, A., and Bureau, M. 2004, *AJ*, 127, 3192
- de Vaucouleurs, G. 1974, In *Formation and Dynamics of Galaxies*, IAUS No. 58, edited by J.R. Shakeshaft (Reidel, Dordrecht). p. 335
- Debattista V.P., Carollo C., Mayer L., and Moore, B. 2005, *ApJ*, 628, 678
- Debattista V., Mayer L., Carollo M., Moore, B., Wadsley, J., and Quinn, T. 2006, *ApJ*, 645, 209
- Dettmar R., and Barteldress A. 1988, *BAAS*, 20, 1085
- Dwek E., Arendt R. G., Hauser M.G. et al. 1995, *ApJ*, 445, 716
- Eliche-Moral, M. C., González-García, A. C., Aguerri, A. et al. 2013, *A&A*, 552, 67
- Emsellem, E., Cappellari, M., Krajnovic, D., Alatalo, K., Blitz, L., Bois, M., Bournaud, F. et al. 2011, *MNRAS*, 414, 888
- Erwin, P., Beltrán, J., Graham, A., and Beckman, J. E. 2003, *ApJ*, 597, 929
- Erwin, P., and Debattista, V. P. 2013, *MNRAS*, 431, 3060
- Erwin, P., Saglia, R., Fbričius, M. Thomas, J., Nowak, N., Rusli, S., and Bender, R. et al. 2015, *MNRAS*, 446, 4039
- Falcón-Barroso, J., Bacon, R., Bureau, M. et al. 2006, *MNRAS*, 369, 529
- Gadotti, D. 2009, *MNRAS*, 393, 1531
- Ganda, K., Peletier, R., McDermid, R. et al. 2007, *MNRAS*, 380, 506
- Guedes, J., Mayer, L., Carollo, M., and Madau, P. 2013, *ApJ*, 772, 36

- Graham, A. 2011: A review of elliptical and disc galaxy structure, and modern scaling laws, appeared in "Planets, Stars and Stellar Systems", Vol. 6, Springer Publishing
- Hernquist, L., and Quinn, P. J. 1988, *ApJ*, 331, 682
- Jablonska, P., Gorgas, J., and Goudfrooij, P. 2007, *A&A* 474, 763
- Jarvis, B. 1986, *AJ*, 91, 65
- Kormendy, J. 1982, *ApJ*, 257, 75
- Kormendy, J. 1983, *ApJ*, 275, 529
- Kormendy, J., and Illingworth, G. 1982, *ApJ*, 256, 460
- Kormendy, J., and Illingworth, G. 1983, *ApJ*, 265, 632
- Kormendy, J., and Barentine, J. 2010, *ApJL*, 715, 176
- Krajnovic, D., Emsellem, E., Cappellari, M., Alatalo, K., Blitz, L., Bois, M., Bournaud, F. et al. 2011, *MNRAS*, 414, 2923
- Kuijken, K., and Merrifield, M. 1995, *ApJ*, 443, 13
- Lauer, T. 1985, *MNRAS*, 216, 429
- Laurikainen, E., Salo, H., and Buta, R. 2005 *MNRAS*, 362, 1319
- Laurikainen, E., Salo, H., Buta, R., and Knapen, J.H. 2007, *MNRAS*, 381, 401
- Laurikainen, E., Salo, H., Buta, R., Knapen, J.H., and Comerón, S. 2010, *MNRAS*, 405, 1089
- Laurikainen, E., Salo, H., Buta, R., and Knapen, J. H. 2011, *MNRAS*, 418, 1452
- Laurikainen, E., Salo, H., Athanassoula, E., Bosma, A., Buta, R., and Janz, J. 2013, *MNRAS*, 430, 3489
- Laurikainen, E., Salo H., Athanassoula, E., Bosma, A., and Herrera-Endoqui, M. 2014, *MNRAS Letter*, 444, 80
- Li, Z-Y, and Shen, J. 2012, *ApJL*, 757, 7
- de Lorenzo-Cáceres, A., Vazdekis A., Aguerri, J. A. L., Corsini, E. M., and Debattista, V. P. 2012, *MNRAS*, 420, 1092
- Lütticke, R., Dettmar, R., and Pohlen, M. 2000a, *A&AS*, 145, 405
- Lütticke, R. Dettmar, R., and Pohlen, M. 2000b, *A&A*, 362, 435
- Lütticke, R., Pohlen, M., and Dettmar, R. 2004, *A&A*, 417, 527
- MacArthur, L., Lauer, A., González, J., and Courteau, S. 2009, *MNRAS*, 395, 28
- Martinez-Valpuesta, I., Shlosman, I., and Heller, C. H. 2006, *ApJ*, 637, 214
- Martini, P., Regan M., Mulchaey, J., Pogge, R. 2003, *ApJS*, 146, 353
- Méndez-Abreu, J., Corsini, E., Debattista, V. P., De Rijcke, S., Aguerri, J. A. L., and Pizzella, A. 2008, *ApJ*, 679, 73
- Méndez-Abreu, J., Debattista, V. P., Corsini, E. M., and Aguerri, J. A. L. 2014, *A&A*, 572, 25
- Moorthy, B.K., and Holzman, J.A 2006, *MNRAS*, 371, 583
- Patsis, P., Skokos, Ch., and Athanassoula, E. 2002a, *MNRAS*, 337, 578
- Patsis, P., Athanassoula, E., Grosbol, P., Skotos, Ch. 2002b, *MNRAS*, 337, 1049
- Patsis, P., and Katsanikas, M. 2014a, *MNRAS*, 445, 3526
- Patsis, P., and Katsanikas, M. 2014b, *MNRAS*, 445, 3546
- Peletier, R., Falcón-Barroso, J., Bacon, R. Cappellari, M., Davies, R. L., de Zeeuw, P. T., Emsellem, E. et al. 2007, *MNRAS*, 379, 445
- Pérez, I., Sánchez-Blázquez, P., and Zurita, A. 2009 *A&A*, 495, 775
- Pérez, I., and Sánchez-Blázquez, P. 2011 *A&A*, 529, 64
- Pfenniger, D., and Friedli, D. 1991, *A&A*, 252, 75
- Pohlen, M., Balcells, M., Lütticke, R., and Dettmar, R. J. 2004, *A&A*, 422, 465
- Proctor, R., and Sansom, A. 2002, *MNRAS*, 333, 517
- Saha, K., Martinez-Valpuesta, I., and Gerhard, O. 2012, *MNRAS*, 421, 333
- Saha, K., and Naab, T. 2013, *MNRAS*, 434, 1287
- Salo, H., Laurikainen, E., Buta, R., and Knapen, J. H. 2010, *ApJL*, 715, 56
- Salo, H., Laurikainen, E., Laine, J. et al. 2015, *ApJL*, 219:4
- Sánchez-Blázquez, P., Ocvirk, P., Gibson, B. K., Pérez, I., and Peletier, R. F. 2011, *MNRAS*, 415, 709
- Sánchez-Blázquez P., Rosales-Ortega F., Méndez-Abreu, J., Pérez, I., Sánchez, S. F., Zibetti, S., Aguerri, J. et al. 2014 *A&A*, 570, 6

- Sandage A. 1961, *The Hubble Atlas of Galaxies*", 1961, Washington, D.C.: Carnegie Institution of Washington
- Shaw, M., Dettmar, R., and Barteldrees, A. 1990, *A&A*, 240, 36
- Shaw, M. 1993, *A&A*, 280, 33
- Shen, J., Rich, R. M., Kormendy, J., Howard, C. D., De Propriis, R., and Kunder, A. 2010, *ApJL*, 720, 72
- Sheth, K., Regan, M., Hinz, J., Gil de Paz, A., Menéndez-Delmestre, K., Munoz-Mateos, J-C, Seibert, M. et al. 2010, *PASP*, 122, 1397
- Simien, F., and de Vaucouleurs, G. 1986, *ApJ*, 302, 564
- Vega Beltran J. C., Corsini E. M., Pizzella A., Bertola, F. 1997 *A&A*, 324, 485
- Weinzirl, T., Jogee, S., Khochfar S., Burkert, A., and Kormendy, J. 2009, *ApJ*, 696, 411
- Wegg, C., and Gerhard, O. 2013, *MNRAS*, 435, 1874
- Whitmore, B. C., and Bell, M. 1988, *ApJ*, 324, 741
- Williams, M., Zamojski, M., Bureau, M., Kuntschner, H., Merrifield, M.R., de Zeeuw, P.T., and Kuijken, K. 2011 *MNRAS*, 414, 2163
- Williams, M., Bureau, M., and Kuntschner, H. 2012, *MNRAS*, 427, 99
- Yoshino, A., and Yamauchi, C. 2015, *MNRAS*, 446, 3749